Biosorption of effluent organic matter onto magnetic biochar composite: Behavior of fluorescent components and their binding properties

Dong Wei [a], Huu Hao Ngo [b], Wenshan Guo [b], Weiying Xu [a], Yongfang Zhang [a], Bin Du [a]*, Qin Wei [c]

[a] *School of Resources and Environment, University of Jinan, Jinan 250022, PR China*

[b] *School of Civil and Environmental Engineering, University of Technology Sydney, Broadway, NSW 2007, Australia*

[c] *Key Laboratory of Chemical Sensing & Analysis in Universities of Shandong, School of Chemistry and Chemical Engineering, University of Jinan, Jinan 250022, PR China*

Abstract

Effluent organic matter (EfOM) is of great concern as one of main sources of organic pollutants from biologically treated wastewater, which is harmful to the quality of receiving waters. In present study, magnetic biochar composite (MBC) was successfully prepared, characterizated and applied to EfOM treatment. The interaction between EfOM and MBC was explored by a combination of excitation-emission matrix (EEM), parallel factor analysis (PARAFAC), synchronous fluorescence, two-dimensional correlation spectroscopy (2D-COS), and molecular weight distribution. Result implied that two fluorescence components were derived from EEM-PARAFAC, and their relative fluorescence intensity scores expressed decreased trend. Moreover, fluorescence quenching of EfOM with increased MBC took place

* Corresponding author. Tel: +86 531 8276 7370; fax: +86 531 8276 7370.
E-mail address: dubin61@gmail.com (B. Du); weidong506@163.com (D.Wei).

sequentially in the following order: protein-like fraction < fulvic-like and humic-like fractions. Molecular weight distribution suggested that MBC had different uptake ability to different size ranges of EfOM. The obtained results could provide a potential application of fluorescence spectroscopy for EfOM treatment assessment.

Keywords: Effluent organic matter (EfOM); Excitation-emission matrix (EEM); Parallel factor analysis (PARAFAC); Two-dimensional correlation spectroscopy (2D-COS); Synchronous fluorescence spectroscopy.

1. Introduction

Recently, effluent organic matter (EfOM) originating from wastewater treatment plant (WWTP) is of significant concern since it negatively affects the quality of effluent (Henderson et al., 2011). The main components of EfOM are consisting of dissolved natural organic matter, refractory compounds, residual degradable substrate, intermediates, soluble microbial products, and trace harmful chemicals (Barker and Stuckey, 1999). The production of EfOM in biological wastewater treatment are greatly influenced by many operational stress conditions, such as hydraulic shock loads, low pH, nutrient deficiency, and presence of toxic compounds etc (Jarusutthirak and Amy, 2007). It is generally accepted that the deep treatment of EfOM is not only beneficial to meet the strict disposal standards but also an essential strategy for making better reuse of limited water resource. Therefore, various effectiveness of specific EfOM treating processes have been developed in recent years, including flocculation, ion exchange, sorption, biofiltration, advanced oxidation, and membrane

processes (Shon et al., 2006).

Among all above-mentioned methods, sorption is considered as a promising choice for EfOM removal effectively from WWTP effluents aiming at decreasing the pollution of receiving water bodies (Zietzschmann et al., 2014). Biochar, as one of typical kind of low-cost sorbents, has been successfully applied for removing potential organic and inorganic pollutants because of its free availability and high sorption capacity. However, one challenge of the application of biochar is the difficulty to separate and recover it from aqueous solution except by high speed centrifugation or filtration, which means high of operational complexity together with a large amount of energy consumption (Ren et al., 2013). To solve this problem, functionalized magnetic materials have been developed in the field of wastewater treatment to overcome the recovery of adsorbents from treated aqueous solution (Jin et al., 2015). Compared with conventional separation methods, the advantage of magnetic nanoparticles is easy to combine with magnetic field to achieve rapid magnetic separation (Mohan et al., 2011). Therefore, it is expected that the combination use of biochar and magnetic separation would have a well prospect in advanced treatment of EfOM in practical application.

Since the components of EfOM are complicated, many analytical methods have been developed and applied to reveal the EfOM removal mechanism during advanced treatment process, including ultraviolet/visible spectrometry (UV/Vis), fluorescence spectroscopy, Fourier-transform infrared spectroscopy (FTIR) and nuclear magnetic resonance (NMR) etc (Michael et al., 2015). Fluorescence spectroscopy, including

three-dimensional excitation-emission matrix (3D-EEM) and synchronous fluorescence, has been extensively utilized for characterization the chemical composition, concentration, distribution and dynamics of samples in water and wastewater due to its rapid, selective and sensitive (Ni et al., 2010; Yu et al., 2013). In particular, detailed investigations have been reported on the utilization of parallel factor analysis (PARAFAC) as an effective multivariate data analysis method to deconvolute complex EEMs into independent fluorescent components which represent groups of similar fluorophores (Ishii and Boyer, 2012). Recent research also has demonstrated that two dimensional correlation spectroscopy (2D-COS) could resolve overlapped peaks problem of one-dimensional synchronous fluorescence by extending spectral intensity trends over a second dimension, and thus provide insightful information about the relative directions and sequential orders of structural variations (Xu et al., 2013). Since a significant typical fluorescent components present in aquatic EfOM (e.g., humic and fulvic acids, and proteinaceous material) (Esparza-Soto et al., 2011; Yu et al., 2015), it is of a particular interest for providing a basis of fluorescence analysis and multivariate calibration method as a powerful tool to characterize the binding property of EfOM during sorption process. However, there is still a lack of thorough examination towards this point.

Based on the above discussion, the objective of this study was to investigate the feasibility of EfOM sorption onto magnetic biochar composite (MBC) from wastewater. For this purpose, MBC was synthesized, characterized and applied for EfOM removal in view of sorption contact time, adsorption kinetics and adsorption

isotherm. A combined use of 3D-EEM, PARAFAC, synchronous fluorescence, 2D-COS, and molecular weight distribution were employed to elucidate the interaction between EfOM and MBC. The obtained results could provide insightful information to select, design and optimize the WWTP effluent treatment facilities by considering the point of spectroscopy characterization.

2. Materials and methods

2.1 Effluent organic matter sample

EfOM sample was collected from the secondary settling tank of a municipal WWTP in Jinan, Shandong province, China. The WWTP was treated by using Anaerobic-Anoxic-Oxic (A^2/O) activated sludge process with a treatment capacity of 20,000 m^3/day. The sample was filtered through a 0.45 nm filter, and next stored at 4 ^oC until use. Total organic carbon (TOC) of the collected EfOM sample is typically around 9.0 mg/L with pH at about 7.5.

2.2 Synthesis of magnetic biochar composite

Biochar was carbonized by using shell as raw material. MBC was prepared by using co-precipitation method (Mohan et al., 2011), and the detailed procedure was as follows: Firstly, 50 g biochar was suspended in a beaker with 500 mL of deionized water. Then, 18 g $FeCl_3$ and 20 g $FeSO_4$ were sequentially added to another beaker with 1500 mL of deionized water and stirred until they were dissolved completely. Next, both solutions were mixed and stirred at 60-70 ^oC for 20 min. Thereafter, 10 M-NaOH (aqueous) was added drop wise into the mixed suspension until the pH was

10-11. After mixing for 1 h, the suspension was aged at room temperature for 24 h and filtered. The remaining solid particles were repeatedly washed with deionized water followed by ethanol. Finally, the prepared MBC was dried at 50 ^{o}C for 12 h in a hot air oven.

2.3 Batch sorption experiment

For sorption kinetic experiment, about 30 mg of MBC was added into a 150 mL conical flask containing 50 mL EfOM solution and 50 mL deionized water (TOC about 4.5 mg/L). The initial pH value of the mixed solution was adjusted to 7.0 by using 0.1 mol/L HCl or NaOH. The samples were taken at different time intervals in the range of 0 - 45 h and analyzed for their TOC concentrations. TOC was selected as a surrogate parameter because it was wildly used for the quantification of EfOM (Michael et al., 2015). The sorption isotherm was carried out with EfOM varied different initial TOC concentrations (3.5-9 mg/L) onto MBC (10 mg) at pH 7.0 for 48 h to ensure equilibrium.

2.4 EEM-PARAFAC

As for the adsorption capacity analysis for batch kinetic experiment, the suspensions were measured to obtain a time-dependent 3D-EEM. 3D-EEM of excitation wavelength were subsequently scanned from 200 to 400 at 10 nm increments by varying the emission wavelength from 280 to 550 nm at 0.5 nm increments, respectively. A 290 nm emission cutoff filter was used in scanning to eliminate second order Raleigh light scattering. The scanning speed was set at 1200

nm/min for all the fluorescence measurements. PARAFAC was performed to interpret the EEM fluorescence data (n=9). PARAFAC analysis was conducted using MATLAB 7.6 (Mathworks, Natick, MA, USA) with the N-way toolbox (Andersson and Bro, 2000). Prior to modeling, first-order Rayleigh and Raman light scattering in EEM data was removed by using interpolation method (Bahram et al., 2006).

2.5 Synchronous fluorescence spectra and 2D-COS

Before the binding test, 100 mL EfOM sample with initial TOC about 4.5 mg/L was added into each erlenmeyer flask by varying different MBC concentration from 50 to 450 mg/L at pH 7.0 for 48 h before spectral analysis. Prior to 2D analysis, synchronous fluorescence was measured by ranging the excitation wavelengths from 250 to 550 nm with a constant offset ($\Delta\lambda$) of 60 nm (Hur et al., 2011), and thus a set of dose-dependent synchronous fluorescence spectra were obtained.

2D-COS was employed to synchronous fluorescence spectra with the increased MBC concentration as the external perturbation. Two types of the maps, including synchronous (Φ) and asynchronous (Ψ) correlation spectroscopy, can be generated from 2D-COS and mathematically written as follows (Noda and Ozaki, 2004):

$$\Phi(x_1, x_2) = \frac{1}{T_{\max} - T_{\min}} \int_{T}^{T_{\max}} \tilde{y}(x_1, t) \cdot \tilde{y}(x_1, t)\, dt \quad (1)$$

$$\Psi(x_1, x_2) = \frac{1}{T_{\max} - T_{\min}} \int_{T}^{T_{\max}} \tilde{y}(x_1, t \cdot \tilde{z}((x_2, t)\, dt) \quad (2)$$

The parameters of x and t are a spectral variable (i.e., wavelengths) and an external perturbation, respectively. $\tilde{y}(x_1, t)$ is the dynamic spectrum, and $\tilde{z}(x_2, t)$ is

149 the Hilbert-transformed orthogonal spectrum. More detailed information on the
150 mathematical procedures associated to 2D-COS could be found elsewhere (Noda and
151 Ozaki, 2004).

152 *2.6 Analytical methods*

153 The morphology, physical structure and chemical property of prepared MBC
154 were characterized by using Brunauer-Emmett-Teller (BET), FTIR, Scanning electron
155 microscope with energy-dispersive X-ray (SEM-EDX) and Zeta potential, as similarly
156 reported by Mohan et al. (2011). Surface area measurements were performed on
157 Micromeritics ASAP 2020 surface area and porosity analyzer (Quantachrome, United
158 States). FTIR was measured by using a Perkin-Elmer Spectrum One FTIR
159 spectrometer (United States) in the spectral range of 4000-400 cm^{-1}. The surface
160 physical morphology and corresponding element of MBC was obtained by using
161 SEM-EDX (Quanta 250 FEG). Zeta potential was measured by using a Malvern zeta
162 meter (Zetasizer 2000). All fluorescence spectra of EfOM samples were measured
163 using a luminescence spectrometer (LS-55, Perkin-Elmer Co., USA). Molecular
164 weight distribution of EfOM samples was measured by using high performance size
165 exclusion chromatography method and detected by high performance liquid
166 chromatography system (Waters 1525, Waters, USA). TOC was analyzed by using by
167 TOC analyzer (TOC-LCPN, Shimadzu Co., Japan). The adsorption experimental
168 results of TOC were analyzed in triplicate, and the averaged data were presented here.

169 **3. Results and discussion**

3.1 Characterization of MBC

The characterization results of Brunauer-Emmett-Teller (BET), FTIR, SEM, EDX and Zeta potential of the prepared MBC are given in Fig. S1. According to the data, Barrett-Joyner-Halenda (BJH) desorption cumulative volume of pores and BET surface area of MBC is 0.3782 cm^3/g and 359.7 m^2/g, respectively (Fig. S1A). FTIR spectrum demonstrates the presence of N-H at 3130 cm^{-1}, C=O at 1630 cm^{-1} and C-OH at 1400 cm^{-1} in both biochar and MBC (Fig. S1B). However, two main additional peaks were observed at 579 and 880 cm^{-1} in MBC, assigning to the stretching vibrations of Fe-O and C-H out of plane deformation vibration during magnetization process.

The surface physical morphology of MBC was measured by SEM (Fig. S1C). Different shapes of pores were observed on the carbons' surface after magnetic process, which was beneficial for surface adsorption. The corresponding EDX spectrum (Fig. S1D) further proved the existence of iron, sulfur and oxygen on the surface of composite, implying that MBC was successfully prepared from the raw carbonaceous material. Fig. S1E shows that Zeta potentials of MBC declined from 36.0 to -32.8 mV in the pH range of 2-10, respectively. The negative Zeta potential (pH>5.0) of the magnetic production implied that the positively charged pollutants in EfOM may be more easily adsorbed.

3.2 Effect of contact time on EfOM removal

Fig. 1 shows the effect of contact time on EfOM sorption onto MBC. It is

obvious seen that EfOM adsorbed rapidly and amounted to 51.8 % after contact time of 11 h, while 62.9 % of EfOM was uptake by a long period of 45 h to equilibrium. The fast EfOM sorption at the initial stage may be due to the fact that a large number of surface sites are available on MBC. After a lapse of time, it took long time to reach equilibrium because the remaining surface sites were difficult to be occupied due to the repulsion between the solute molecules of the solid and bulk phases (Ahmad and Rahman, 2011).

In present study, four common kinetic models in terms of pseudo-first order, pseudo-second-order, Bangham, and Elovich kinetic models were used to analyze the adsorption kinetics data of EfOM onto MBC. Detailed description of the above four kinetic models could be found in Supplementary material. Table S1 displayed the modeled results of kinetics were calculated based on TOC concentrations. It is concluded that pseudo-first order model and pseudo-second order model have higher correlation coefficients (R^2=0.9497 and 0.9784, respectively). The result implied that physical and chemical sorption were both important during EfOM sorption onto MBC. It has been well reported that EfOM contains different types of organic substances (e.g. endocrine disrupting chemicals (EDCs), pharmaceuticals and personal care products residues (PPCPs) etc.). Therefore, it is possible that physical and chemical adsorption takes place when it comes in contact with activated carbon (Shon et al., 2006).

3.3 Adsorption isotherm

In present study, three common models including Langmuir, Freundlich and Henry equations are described for predicting isotherm results, as shown in Fig. 2. Data implied that the adsorption amount of EfOM onto MBC significantly increased with increasing initial EfOM concentrations. The more description of the maximum adsorption amount (q_m), correlation coefficient (R^2), and the other parameters for all the isotherms are presented in Table S2.

Experimental adsorption data showed a better fit to both Langmuir and Freundlich models (R^2=0.9531 and 0.9137, respectively) than Henry model (R^2=0.8608), suggesting that the above two isotherm models reasonably explain the adsorption behaviors. In previous literatures, Langmuir model was predominantly used to describe sorption of natural organic matter onto carbon nanotubes (CNTs) (Lu and Su, 2007). However, a good fit to Freundlich model was also observed during the adsorption of DOM onto granular-activated carbon (GAC) as a pretreatment to reverse osmosis (RO) desalination of membrane bioreactor (MBR) effluents (Gur-Reznik et al., 2008). As shown in Table S2, the calculated maximum adsorption capacity from Langmuir model is of 56.1 mg/g for MBC, proving its great potential as an effective adsorbent for treating EfOM from biologically treated effluent. The value of $0.1<1/n<1.0$ in Freundlich model implied that adsorption of EfOM onto MBC is favorable, as similarly reported by Sun et al (2008).

3.4 EEM spectra

Fig. 3 shows the EEM spectra of the interaction between EfOM and MBC at

various reaction times from 0 to 20 h. Table S3 summarizes the detailed fluorescence spectral parameters of all EfOM samples, including peak location and fluorescence intensity. As shown in Fig. 3A, four main fluorescence peaks (Peak A, B, C and D) were identified from the 3D-EEM spectroscopy in the raw EfOM sample. Peak A and Peak B were indentified at excitation/emission (Ex/Em) of 230/354 nm and 280/350 nm, respectively, which were related to aromatic protein-like and tryptophan protein-like substances (Wang et al., 2009). There is evidence that the presence of protein-like substances may be attributed to aromatic amino acids and/or tannin-like structures (Hur et al., 2011). Peak C was located at Ex/Em of 330/427.5 nm, which was assigned to humic acid-like substances with regard to a biological production and activity of microorganisms, as similarly reported by Yu et al., (2013). Peak D was observed at Ex/Em of 240/425 nm, which was related to fulvic acid-like substances.

Along with contact time increased, not only fluorescence intensity but also fluorescence peak location in all EfOM samples changed with different degrees, indicating the gradually interaction between EfOM and MBC during sorption process. More detailed, the intensities of all fluorescent peaks approximately decreased by 52.9-67.7 % in the first 5 min, and thereafter those decreased slowly (Table S3), which was consistent with the rapid uptake in the initial sorption process (Fig. 1). It has also been well reported that Peak B and Peak C were representative of the biodegradable and nonbiodegradable components in EfOM samples, respectively (Wang et al., 2009). In present study, the intensity ratio of Peak B/Peak C increased from 0.69 to 1.02, implying that nonbiodegradable component was more easily

adsorbed by MBC and the treated EfOM became more biodegradable. By contrast, Liu et al. (2011) observed that the intensity ratio of Peak B/Peak C decreased in a submerged membrane bioreactor (MBR) with pre-ozonation, suggesting that the biodegradable DOM with fluorescence was gradually metabolized by microorganism. An obvious blue-shift in terms of emission wavelength was observed in Peak C, implying the chemical composition changes during treatment process (Rodríguez et al., 2014).

3.5 PARAFAC analysis

According to PARAFAC analysis, two components were found out to be suitable number by using core consistency diagnostic (close to 100 %) in PARAFAC solution, as shown in Fig. 4. According to the protocol reported by Chen et al. (2003), Component 1 was comprised of two peaks at Ex/Em of 240/435.5 nm and 330/435.5 nm, which represented to fulvic-like substances and humic-like substances. Correspondently, the fluorophore of component 2, with two peaks at Ex/Em of 230/347.5 nm and 280/347.5 nm, were related to protein-like substances. Protein-like substances may be categorized as the mixture of biological matters in PARAFAC analysis, as similarly reported by Ou et al. (2014). PARAFAC analysis also gives the relative fluorescence intensity scores of two components as a function of reaction time, as shown in Fig. 5. Component 1 decreased with much larger degree (0.82 to 0.10) than that of Component 2 (0.70 to 0.14), suggesting that humic-like substances and fulvic-like substances were removed to a much higher extent than that of protein-like

substances.

Applications of combined EEM-PARAFAC analysis has been wildly reported to a variety of environment samples including DOM, soluble microbial products, and extracellular polymeric substances, as compared and displayed in Table S4. Yu et al. (2010) suggested that EEM-PARAFAC could be applied as a valuable research tool for sludge dewaterability, given its high sensitivity, selectivity and simultaneous determination of protein-like, humic acid-like and fulvic acid-like substances. Li et al. (2014) investigated the chemical changes of DOM during anaerobic digestion of dewatered sewage sludge by using EEM-PARAFAC, implying that three fluorescent components indentified and increased relating to tyrosine-like, tryptophan-like and humic-like groups in DOM samples. Wu et al. (2011) evaluated heavy metal binding potential of dissolved organic matter in municipal solid waste leachate through EEM quenching combined with PARAFAC analysis, suggesting that PARAFAC model provided quantitative information regarding on the distribution of fluorescence components. The result of this study further extended the application of EEM-PARAFAC model to EfOM treatment process assessment, which was beneficial to improve and optimize the parameter of advanced treatment process in the future.

3.6 Synchronous fluorescence

Fig. S2 shows the changes in synchronous fluorescence spectra of interaction between EfOM and MBC. Three main regions could be assigned to protein-like, fulvic-like, and humic-like fluorescence fractions corresponding to the wavelength

297 ranges of 250-300, 300-380, and 380-550 nm, respectively (Chen et al., 2015). It was
298 observed that fluorescence intensities were consistently quenched over the whole
299 wavelengths with the addition of MBC. Specifically, a much higher extent of
300 fluorescence quenching of fulvic-like fluorescence peak (342.5 nm) was observed,
301 compared with the shoulder of protein-like fluorescence peak (289 nm). The result of
302 synchronous fluorescence spectra clearly reflected the binding ability between EfOM
303 and MBC, which was consistent with the analysis from 3D-EEM.

304 *3.7 2D-COS*

305 2D-COS analysis was performed to clarify the transformation sequence of
306 various spectral regions with increased MBC addition, and the result is displayed in
307 Fig. 6. One positive auto-peak centering at 342.5 nm was observed along the diagonal
308 line of the synchronous map (Fig. 6A), implying that the occurrence of the spectral
309 changes at the corresponding wavelength region in one direction, as similarly reported
310 by Hur et al. (2011). It was also suggested that fulvic-like fluorescence fraction was
311 more susceptible to the decrease of the fluorescence intensity upon the presence of
312 MBC.

313 In contrast, asynchronous map reveals the sequential or successive changes of
314 the spectral intensities in response to MBC addition. Two negative areas with
315 cross-peaks at 279/300, 279/352, 330/352, 330/389 nm and one positive area
316 centering at 300/330 nm, were observed upper the diagonal line of EfOM in
317 asynchronous map (Fig. 6B). Based on Noda's rule (Noda and Ozaki, 2004),

318 fluorescence quenching took place sequentially in the following order: 279 <300
319 <330<352 and 389 nm. The result demonstrated that the longer wavelength exhibited
320 higher binding affinities than that of shorter wavelength. It is suggested that
321 fluorescence quenching took place sequentially in the following order: protein-like
322 fraction < fulvic-like and humic-like fractions. The obtained binding order of EfOM
323 and MBC was in agreement with the result of PARAFAC, implying that 2D-COS
324 could be applied as an effective method to assess the binding property of EfOM onto
325 MBC.

326 *3.8 Molecular weight distribution*

327 In order to better understand the different size ranges of EfOM removal during
328 the advanced treatment process, molecular weight distribution of EfOM samples
329 before and after reaction with MBC was evaluated (Fig. S3). It was obviously
330 observed that the majority of molecular weight fractions decreased with different
331 degrees after reaction with MBC. The higher fraction of organic compound with
332 molecular weight 1200-1500 Da in raw EfOM, which was attributed to the presence
333 of humic and fulvic acids produced in biological treatment process, as similarly
334 reported by Huber and Frimmel (1996). The highest removal percentage in terms of
335 molecular weight fraction was 77.0 % at 492 Da, suggesting that MBC had the ability
336 for treating emerging contaminants including Endocrine Disrupting Chemicals (EDCs)
337 and Pharmaceutical and Personal Care Products (PPCPs) in low molecular weight
338 range from 100 to 500 Da (Shon et al., 2006). Jarusutthirak and Amy (2007) also

reported that small molecules with molecular weight between 100 and 200 Da was related to low molecular weight organic acids, amino acids, or simple sugars which were possibly produced during biomass growth. Therefore, the result of high performance size exclusion chromatography implied that the binding ability and removal efficiency of various size ranges WWTP effluent onto MBC was different.

4. Conclusions

In summary, EfOM sorption onto MBC followed pseudo-second order kinetic model and the adsorption isotherm data could be described with Langmuir and Freundlich models. Two components of EfOM were identified from EEM-PARAFAC model and the relative fluorescence intensity scores of two components decreased as a function of reaction time. Synchronous fluorescence spectra and 2D-COS analysis reflected the different binding property between EfOM fractions and MBC with the following order: protein-like < fulvic-like and humic-like fractions. The result of this study is helpful to provide insightful information with respect to EfOM treatment process regarding to the point of spectroscopy characterization.

5. Acknowledgements

This study was supported by the National Natural Science Foundation of China (21377046), Special project of independent innovation and achievements transformation of Shandong Province (2014ZZCX05101), Science and technology development plan project of Shandong province (2014GGH217006), Shanghai Tongji Gao Tingyao Environmental Science & Technology Development Foundation

(STGEF) and QW thanks the Special Foundation for Taishan Scholar Professorship of Shandong Province and UJN (No.ts20130937).

References

[1] Ahmad, M.A., and Rahman, N.K., 2011. Equilibrium, kinetics and thermodynamic of Remazol Brilliant Orange 3R dye adsorption on coffee husk-based activated carbon. Chem. Eng. J. 170, 154-161.

[2] Andersson, C.A., and Bro, R., The N-way toolbox for matlab. Chemom. Intell. Lab. Syst. 2000, 1-4.

[3] Barker, D.J., and Stuckey, D.C., 1999. A review of soluble microbial products (SMP) in wastewater treatment systems. Water Res. 33, 3063-3082.

[4] Bahram, M., Bro, R., Stedmon, C., Afkhami, A., 2006. Handling of Rayleigh and Raman scatter for PARAFAC modeling of fluorescence data using interpolation. J. Chemom. 20, 99-105.

[5] Chen, W., Habibul. N., Liu. X.Y., Sheng, G.P., Yu, H.Q., 2015. FTIR and Synchronous Fluorescence Heterospectral Two-Dimensional Correlation Analyses on the Binding Characteristics of Copper onto Dissolved Organic Matter. Environ. Sci. Technol. 49, 2052-2058.

[6] Chen, W., Westerhoff, P., Leenheer, J.A., Booksh, K., 2003. Fluorescence excitation-emission matrix regional integration to quantify spectra for dissolved organic matter. Environ. Sci. Technol. 37, 5701-5710.

[7] Esparza-Soto, M., Núñez-Hernández, S., Fall, C., 2011. Spectrometric characterization of effluent organic matter of a sequencing batch reactor operated at three sludge retention times. Water Res. 45, 6555-6563.

[8] Gur-Reznik, S., Katz, I., Dosoretz, C.G., 2008. Removal of dissolved organic matter by granular-activated carbon adsorption as a pretreatment to reverse osmosis of membrane bioreactor effluents. Water Res. 42, 1595-1605.

[9] Henderson, R.K., Subhi, N., Antony, A., Khan, S.J., Murphy, K.R., Leslie, G.L., Chen, V., Stuetz, R.M., Le-Clech, P., 2011. Evaluation of effluent organic matter fouling in ultrafiltration treatment using advanced organic characterisation techniques. J. Membr. Sci. 382, 50-59.

[10] Huber, S.A., and Frimmel, F.H., 1996. Size-exclusion chromatography with organic carbon detection (LC-OCD): a fast and reliable method for the characterization of hydrophilic organic matter in natural waters. Vom Wasser. 86, 277-290.

[11] Hur, J., Jung, K.Y., Jung, Y.M. 2011. Characterization of spectral responses of humic substances upon UV irradiation using two-dimensional correlation spectroscopy. Water Res. 45, 2965-2974.

[12] Ishii, S.K., and Boyer, T.H., 2012. Behavior of reoccurring PARAFAC components in fluorescent dissolved organic matter in natural and engineered systems: a critical review. Environ. Sci. Technol. 46, 2006-2017.

[13] Jarusutthirak, C., and Amy, G., 2007. Understanding soluble microbial products (SMP) as a component of effluent organic matter (EfOM). Water Res. 41, 2787-2793.

[14] Jin, Z.X., Wang, X.G., Sun, Y.B., Ai, Y.J., Wang, X.K., 2015 Adsorption of 4-n-nonylphenol and bisphenol-A on magnetic reduced graphene oxides: a combined experimental and theoretical studies. Environ. Sci. Technol. 49, 9168-9175.

[15] Li, X., Dai, X., Takahashi, J., Li, N., Jin, J., Dai, L., Dong, B., 2014. New insight into chemical changes of dissolved organic matter during anaerobic digestion of dewatered sewage sludge using EEM-PARAFAC and two-dimensional FTIR correlation spectroscopy. Bioresour. Technol. 159, 412-420.

[16] Liu, T., Chen, Z.L., Yu, W.Z., You, S.J., 2011. Characterization of organic membrane foulants in a submerged membrane bioreactor with pre-ozonation using three-dimensional excitation-emission matrix fluorescence spectroscopy. Water Res. 45, 2111-2121.

[17] Lu, C., and Su, F., 2007. Adsorption of natural organic matter by carbon nanotubes, Sep. Purif. Technol. 58, 113–121.

[18] Michael, I., Michael, C., Duan, X., He, X., Dionysiou, D., Mills, M. and Fatta-Kassinos, D., 2015. Dissolved effluent organic matter: Characteristics and potential implications in wastewater treatment and reuse applications. Water Res. 77, 213-248.

[19] Mohan, D., Sarswat, A., Singh, V.K., Alexandre-Franco, M., Pittman, C.U., 2011. Development of magnetic activated carbon from almond shells for trinitrophenol removal from water. Chem. Eng. J. 172, 1111-1125.

[20] Ni, B.J., Zeng, R.J., Fang, F., Xie, W.M., Sheng, G.P., Yu, H.Q., 2010. Fractionating soluble microbial products in the activated sludge process. Water Res. 44, 2292-2302.

[21] Noda, I.; Ozaki, Y., 2004. Two-dimensional correlation spectroscopy: applications in vibrational and optical spectroscopy. John Wiley and Sons Inc., London.

[22] Ou, H.S., Wei, C.H., Mo, C.H., Wu, H.Z., Ren, Y., Feng, C.H., 2014. Novel insights into anoxic/aerobic/aerobic biological fluidized-bed system for coke wastewater treatment by fluorescence excitation-emission matrix spectra coupled with parallel factor analysis. Chemosphere. 113, 158-164.

[23] Ren, Y., Abbood, H.A., He, F., Peng, H., Huang, K., 2013. Magnetic EDTA-modified chitosan/SiO_2/Fe_3O_4 adsorbent: preparation, characterization, and application in heavy metal adsorption. Chem. Eng. J. 226, 300-311.

[24] Rodríguez, F. J., Schlenger, P., García-Valverde, M., 2014. A comprehensive structural evaluation of humic substances using several fluorescence techniques before and after ozonation. Part I: Structural characterization of humic substances. Sci. Total Environ. 476-477, 718-730.

[25] Shon, H., Vigneswaran, S., Snyder, S., 2006. Effluent organic matter (EfOM) in wastewater: constituents, effects, and treatment. Crit. Rev. Env. Sci. Technol. 36, 327-374.

[26] Sun, X. F., Wang, S. G., Liu, X. W., Gong, W. X., Nan, B., Gao, B. Y., 2008. Competitive biosorption of zinc (ii) and cobalt (ii) in single- and binary-metal systems by aerobic granules. J. Colloid Interface Sci. 324, 1-8.

[27] Wang, Z., Wu, Z., Tang, S., 2009. Characterization of dissolved organic matter in a submerged membrane bioreactor by using three-dimensional excitation and emission matrix fluorescence spectroscopy. Water Res. 43, 1533-1540.

[28] Wu, J., Zhang, H., He, P.J., Shao, L.M., 2011. Insight into the heavy metal binding potential of dissolved organic matter in MSW leachate using EEM quenching combined with PARAFAC analysis. Water Res. 45, 1711-1719.

[29] Xu, H.C., Jiang, H.L., 2013. UV-induced photochemical heterogeneity of dissolved and attached organic matter associated with cyanobacterial blooms in a eutrophic freshwater lake. Water Res. 47, 6506-6515.

[30] Yu, G.H., He, P.J., Shao, L.M., 2010. Novel insights into sludge dewaterability by fluorescence excitation-emission matrix combined with parallel factor analysis. Water Res. 44, 797-806.

[31] Yu, H.R., Qu, F.S., Sun, L., Liang, H., Han, Z.S., Chang, H.Q., Shao, S.L., Li, G.B., 2015. Relationship between soluble microbial products (SMP) and effluent organic matter (EfOM): Characterized by fluorescence excitation emission matrix coupled with parallel factor analysis. Chemosphere. 121, 101-109.

[32] Yu, H., Song, Y., Tu, X., Du, E., Liu, R., Peng, J., 2013. Assessing removal efficiency of dissolved organic matter in wastewater treatment using fluorescence excitation emission matrices with parallel factor analysis and second derivative synchronous fluorescence. Bioresour. Technol. 144, 595-601.

[33] Zietzschmann, F., Worch, E., Altmann, J., Ruhl, A.S., Sperlich, A., Meinel, F., Jekel, M., 2014. Impact of EfOM size on competition in activated carbon adsorption of organic micro-pollutants from treated wastewater. Water Res. 65, 297-306.

Figure Captions

Fig. 1 Effect of contact time on EfOM sorption onto MBC.

Fig. 2 Sorption isotherms fit of EfOM onto MBC with different initial EfOM concentrations.

Fig. 3 EEM spectra of the interaction between EfOM and MBC at various reaction times.

Fig. 4 Two components identified by PARAFAC based on EEM spectra of the EfOM samples: (A) Component 1; (B) Component 2.

Fig. 5 Fluorescence intensity scores of two PARAFAC-derived components in nine EfOM samples as a function of reaction time.

Fig. 6 2D-COS maps for the synchronous fluorescence spectra of interaction between EfOM and MBC: (A) synchronous map; (B) asynchronous map.

486

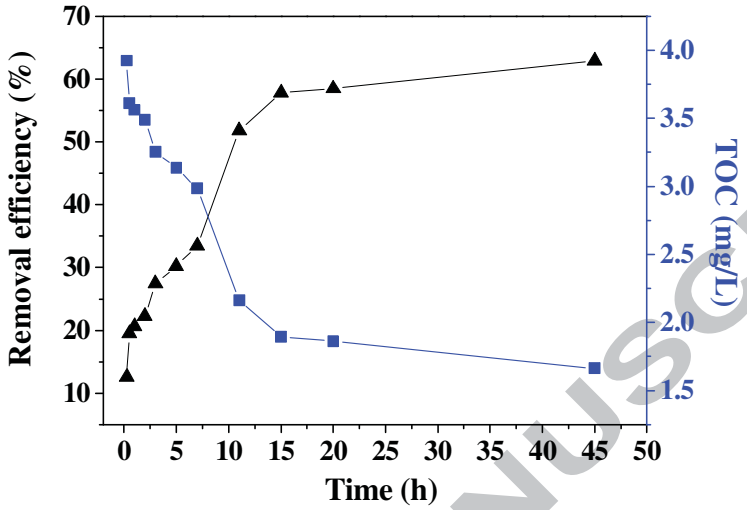

487

488 **Fig. 1** Effect of contact time on EfOM sorption onto MBC.

489

490

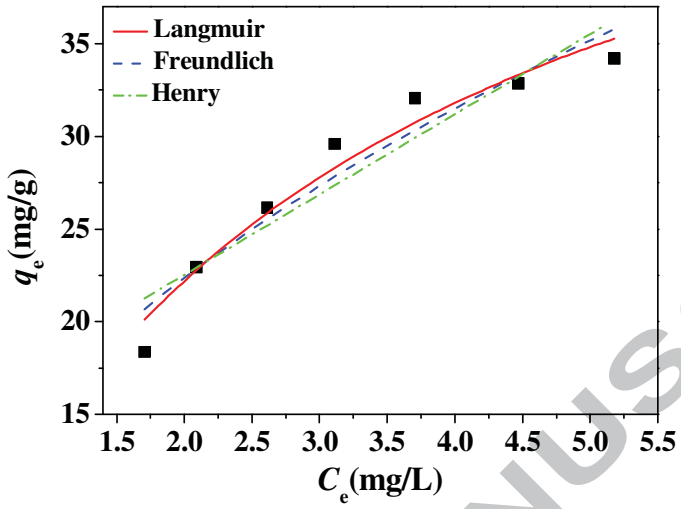

491

492 **Fig. 2** Sorption isotherms fit of EfOM onto MBC with different initial EfOM

493 concentrations.

494

495

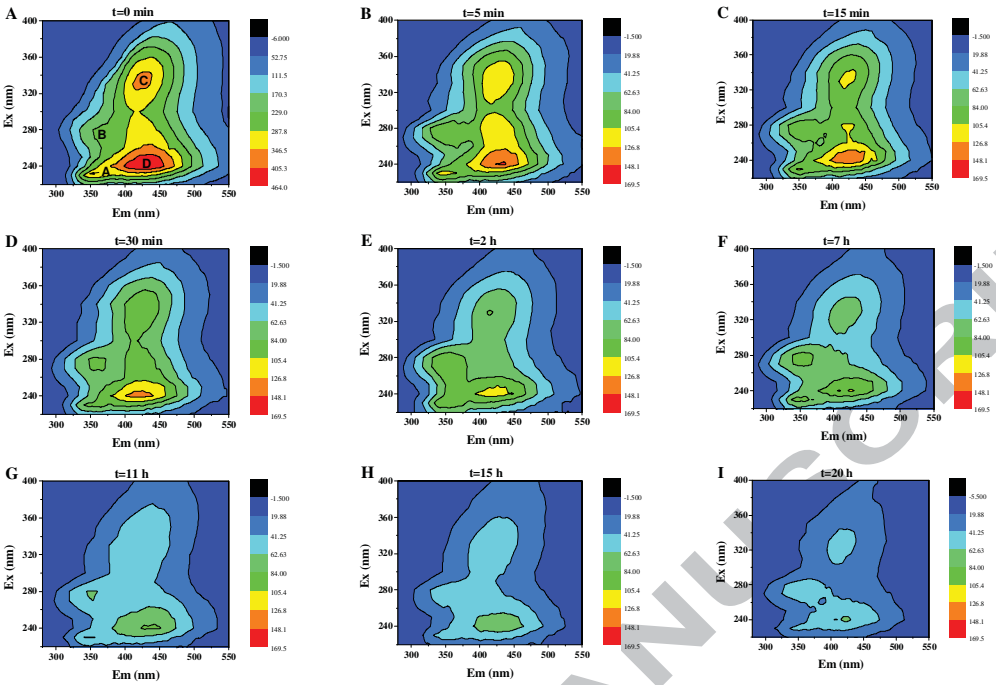

496 **Fig. 3** EEM spectra of the interaction between EfOM and MBC at various reaction

497 times.

498

499

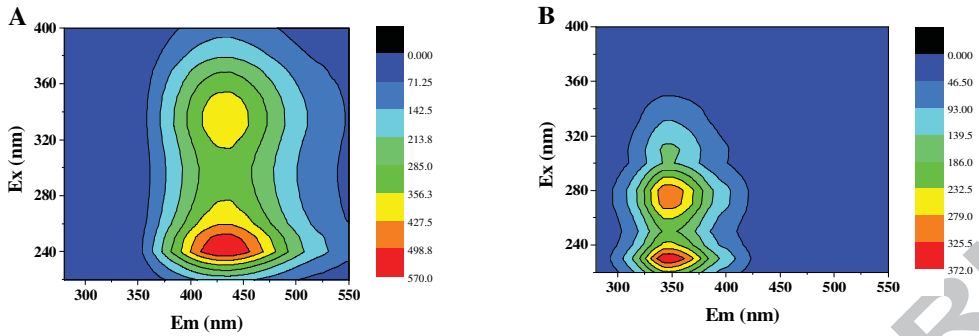

500 **Fig. 4** Two components identified by PARAFAC based on EEM spectra of the EfOM
501 samples: (A) Component 1; (B) Component 2.

502

503

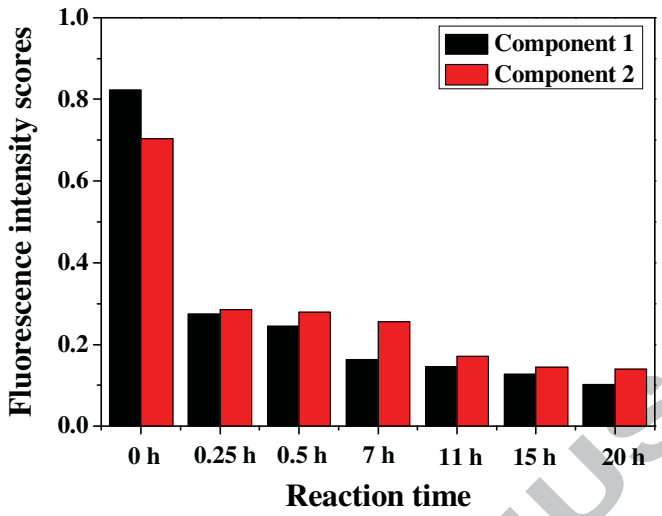

504

505 **Fig. 5** Fluorescence intensity scores of two PARAFAC-derived components in nine

506 EfOM samples as a function of reaction time.

507

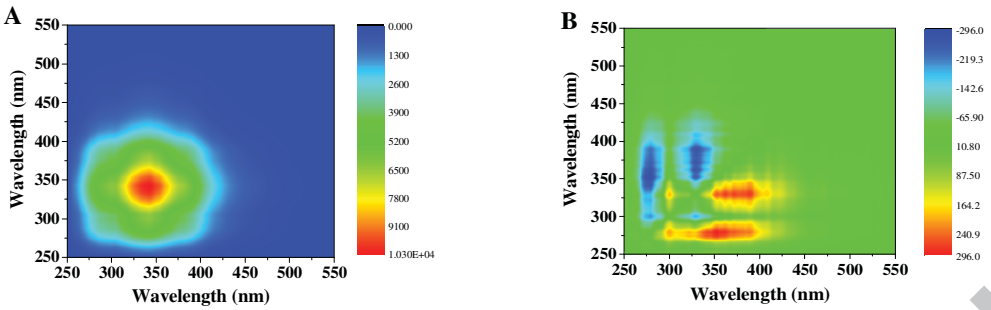

508 **Fig. 6** 2D-COS maps for the synchronous fluorescence spectra of interaction between

509 EfOM and MBC: (A) synchronous map; (B) asynchronous map.

510

511

512

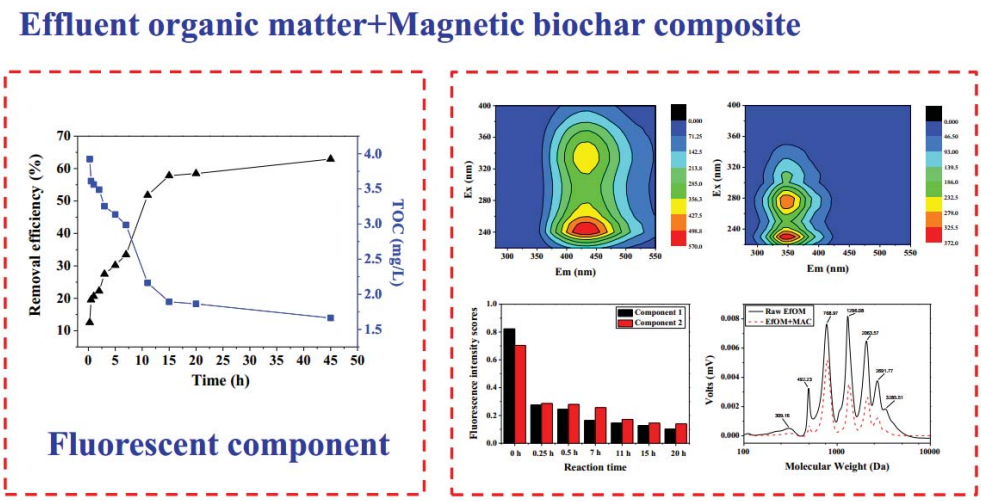

513

514

515 Graphical abstract

516

517

518 **Research Highlights**

519 ➢ MBC was successfully prepared, characterized and applied for treating EfOM.

520 ➢ Fluorescent components of EfOM were identified by using EEM-PARAFAC.

521 ➢ Fluorescence quenching order of EfOM onto MBC was obtained from 2D-COS.

522 ➢ The majority of EfOM in terms of MW were removed with different degrees.

523